

24. We assumed that the quasiparticle multiplication factor is 100, which is similar to that used in Ref. 16.
25. P. H. Ballentine, A. M. Kadin, and D. S. Mallory, *IEEE Trans. Magn.* **27**, 997 (1991).
26. S. Witanachchi *et al.*, *Appl. Phys. Lett.* **53**, 234 (1988).
27. J. R. Gavaler *et al.*, *J. Appl. Phys.* **70**, 4383 (1991).
28. P. H. Ballentine, A. M. Kadin, M. A. Fisher, D. S. Mallory, and W. R. Donaldson, *IEEE Trans. Magn.* **25**, 950 (1989).
29. Photovoltage measurements [A. D. Semenov *et al.*, *Appl. Phys. Lett.* **60**, 903 (1992)] confirm that YBCO is indeed in the normal state under an optical excitation at the level used in our measurements.

## **2.B Increased Retention Time for Hydrogen and Other Gases by Polymer Shells Using Optically Transparent Aluminum Layers**

A key difficulty in fabricating fuel capsules with polymer walls for inertial fusion is the high permeability of most polymers to the hydrogen isotopes used as fuel gases. In this article, it is shown that a thin aluminum layer can increase the retention time of a polymer shell for  $D_2$  from several minutes to several hours, while remaining transparent enough to allow interferometric measurement of changes in gas content. Having achieved a time constant for gas retention of an hour or more, a shell can be filled with fuel gas (along with a diagnostic gas such as Ar or Ne), and the Al layer thickened before a significant amount of the gas permeates out. This thicker Al layer greatly increases the time constant, but being opaque, prevents further interferometric characterization. Because many days may elapse before the capsule is used in an inertial-fusion experiment, slow loss of fuel is prevented by storing the capsule in pressurized fuel gas until the day of use.

Polymer shells are desirable fuel capsules for inertial-fusion experiments because they are composed of elements with low atomic number.<sup>1</sup> Spherical shells with the necessary high degree of uniformity may be fabricated by starting with polystyrene (PS) shells made by the microencapsulation<sup>2,3</sup> or drop-tower method,<sup>4</sup> and the walls uniformly thickened with another polymer by bouncing the shells during the coating process.<sup>5-7</sup> Prior to this study, the only method available for increasing the time constant for gas retention that still allowed interferometric characterization was to coat the shells with a thin layer of polyvinyl alcohol (PVA) or to incorporate such a layer between two of the other polymers. While the PVA layer can greatly increase the time constant for gas retention, this property can be significantly degraded by exposure of the PVA to beta radiation from tritium decay.<sup>8</sup> There is no reason to expect that similar degradation would occur with Al barrier layers.

In this study, PS shells are made by the microencapsulation method, selected for wall thickness and uniformity using optical interferometry, and the walls thickened with parylene while the shells are bounced. The shells are then glued to single support stalks of small diameter (4  $\mu\text{m}$ ) and coated with a thin layer of Al (45  $\text{\AA}$  to 140  $\text{\AA}$ ) using a dc sputter source while being rotated under the source. The shells are then permeated with  $\text{D}_2$ , or a diagnostic gas such as Ar or Ne. Since the shells are still partially transparent, the shells can be placed in an interferometer, and the change in pressure measured as a function of time. After determination of the gas-retention time constant(s) for the gas(es) to be used, the shells are permeated to the desired pressure. A time constant of one or more hours allows the shells to be removed from the permeator and coated with additional Al without significant loss of gas. A thickness of 500  $\text{\AA}$  of Al greatly increases the time constant while also serving as a “shinethrough” barrier that prevents preheat of the fuel by the leading edge of the laser pulse during inertial-fusion experiments.

The existing data on permeability of Al to hydrogen isotopes<sup>9</sup> indicate that no significant permeation through the Al occurs, so the gas must be passing through discontinuities in the film. The rate of permeation observed in this study is eight to nine orders of magnitude larger than would be expected if the mechanism of permeation was similar to that of bulk Al. Characterization of the Al film and its discontinuities is beyond the scope of this study, except to note that the film is highly smooth and optically reflective and adheres well to the shell. It is also to be noted that measurements of gas permeating out of these shells show the pressure decreasing exponentially with time, which is characteristic of permeation through a polymer, not a metal.<sup>10</sup> In addition, it is observed that the oxidation of the Al layer, as indicated by an increase in transparency with time, is sometimes accompanied by a significant increase in the observed time constant. It can be speculated that the greater volume of the oxidized layer narrows the discontinuities through which the gas passes. ( $\text{Al}_2\text{O}_3$  with a density of 4.0  $\text{g/cm}^3$  has 30% more volume per Al atom than bulk Al with a density of 2.7  $\text{g/cm}^3$ .)

For thin Al layers, i.e., those with relatively low absorbance, a scanning Fabry-Perot interferometer is used to measure the fill-gas leakage rate through the shells in real time.<sup>11</sup> The technique used is reminiscent of the method by which Fabry-Perot etalons are spectrally tuned by varying the pressure of the gas between the end mirrors and, therefore, the optical path length between them, as opposed to changing their separation.<sup>12,13</sup> For more absorbant layers, a Mach-Zehnder interferometer is used. The pressure  $P$  remaining within the inertial-fusion target after a time  $t$  is

$$P = P_0 e^{-(t-t_0)/\tau} \quad (1)$$

where  $P_0$  is the pressure inside the microballoon at time  $t_0$  and  $\tau$  is the exponential time constant. For a gas,  $n_{\text{gas}}-1$  is directly proportional to the gas pressure within the approximations imposed by both classical theory for the refractive index of rarified media and the ideal-gas law, where  $n_{\text{gas}}$  is the refractive index of the gas. In addition, the phase retardation, or shift, that a wavefront undergoes upon traversing a medium, relative to vacuum, is directly proportional to  $n-1$  for that material.

To interpret the interferometric measurements, the phase shift for light passing through the center of a pressurized shell with respect to light propagating externally to it is expressed as the sum of terms caused by the gas  $\phi_g$  and the shell  $\phi_s$ :

$$\phi = \phi_s + \phi_g \quad (2)$$

The phase shift caused by gas inside the shell is given by

$$\phi_g = m \frac{2r}{\lambda} \frac{P}{P_r} (n_g - 1), \quad (3)$$

where  $P$  is the internal pressure,  $r$  is the gas radius,  $n_g$  is the gas index of refraction at some reference pressure  $P_r$  and wavelength  $\lambda$ , and  $m$  is the number of times the wavefronts that produce the interferogram pass through the shell. For the Mach-Zehnder interferometer  $m = 1$ , while for the Fabry-Perot interferometer  $m = 2$ . The phase shift caused by the shell is

$$\phi_s = m \frac{2w}{\lambda} (n_s - 1), \quad (4)$$

where  $w$  is the wall thickness, and  $n_s$  is the index of refraction of the shell material.

Gas pressure inside the shell causes the shell to expand slightly, stretching and thinning the wall. It will be shown later that this thinning is significant for interferometric measurements. The change in  $\phi_s$  because of thinning is proportional to  $P$  for thin-walled shells, and may be conveniently written as

$$\Delta\phi_s = -\alpha \phi_g, \quad (5)$$

where  $\alpha$  is a constant for a given gas and shell material, and the pressure dependence is contained in  $\phi_g$ .

The gas pressure measured by interferometry may be expressed, combining Eqs. (1)–(5), as

$$P(t) = \frac{[\phi - \phi_{s0}] \lambda P_r}{m 2r (n_g - 1) (1 - \alpha)} = P_0 e^{-(t-t_0)/\tau}, \quad (6)$$

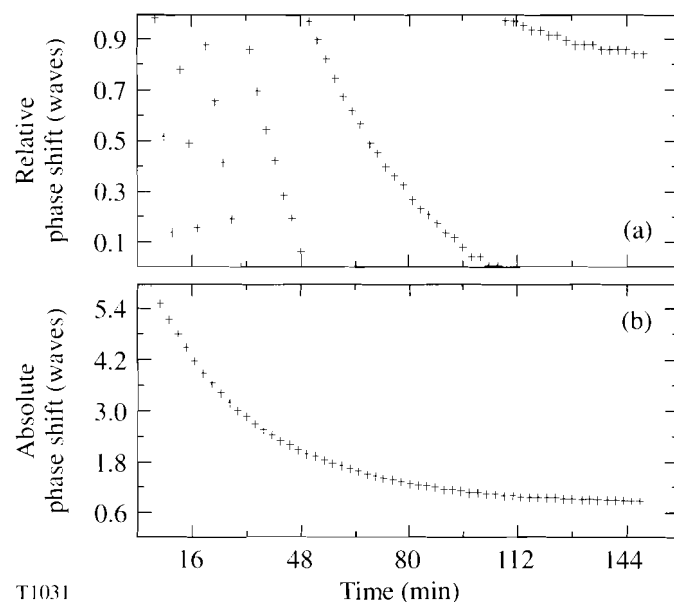
where  $\phi_{s0}$  is the value of  $\phi_s$  when  $P = 0$ . Since monochromatic light is used in each interferometric technique, the absolute phase shift cannot be uniquely determined. The phase shift  $\phi$  consists of an integral part and a fractional part, of which only the fractional component is measured. This fractional component decreases continuously as a function of time, whereas the integral component changes discretely as the fractional part reaches the transition from values greater than zero to those less than 1 as the gas permeates out. When Eq. (6) is fitted to interferometric measurements of  $\phi$  as a function of time, an arbitrary integer value is added to each measurement, and this integer is reduced by 1 each time the value of  $\phi$  makes this transition. A least-squares fit of Eq. (6) to the data generates values of  $\tau$ ,  $P_0$ , and  $\phi_{s0}$ .

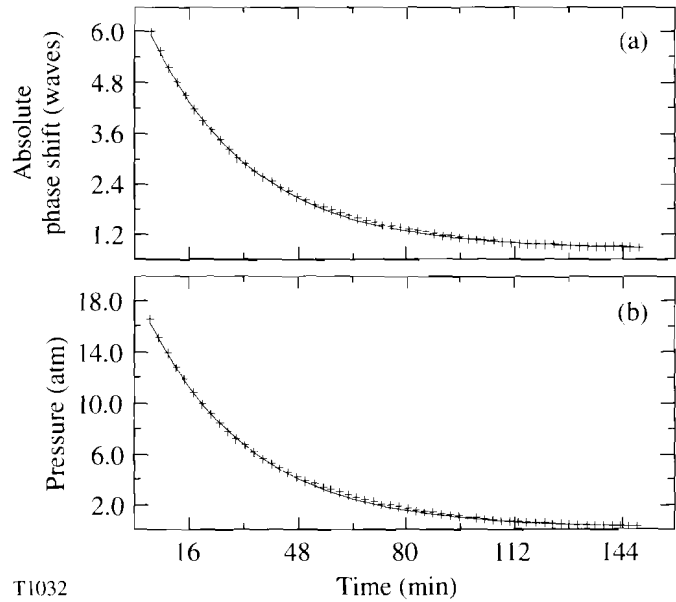
Both the initial pressure inside the shell  $P_0$  and the exponential time constant  $\tau$  are simultaneously measured using a computer and the following method. First, a polymer shell is filled by applying the desired pressure externally to the shell and letting it soak for an appropriate period of time (generally  $t > 5\tau$ ) at room temperature. The external pressure is released and the initial time  $t_0$  is recorded by the data-acquisition computer. The inertial-fusion target is inserted into the scanning Fabry-Perot or Mach-Zehnder interferometer, and individual fractional phase-shift measurements are sequentially recorded along with the elapsed time. A sufficient amount of time is allowed for most of the gas to permeate out of the shell (that is, the phase shift reaches a steady-state value as a function of time), and the data acquisition is terminated. A typical plot of fractional phase shift as a function of elapsed time is shown in Fig. 52.17(a). Integral values are added to each phase-shift value to align them and produce a continuous data set, as illustrated in Fig. 52.17(b). The aligned time-dependent phase-shift values are then least-squares curve fitted to yield a plot such as the one shown in Fig. 52.18(a), and the fitting parameters  $P_0$ ,  $\tau$ ,  $\phi_{s0}$ , and the standard deviation of the fit are determined. (In actuality, initial guesses for  $P_0$ ,  $\tau$ ,  $\phi_{s0}$ , based on the pressure to which the shell was filled and the aligned phase-shift data, are supplied to the curve-fitting routine, and these are numerically adjusted to minimize the standard deviation of the fit.) The fractional phase shift caused by the empty shell  $\phi_{s0}$  is then subtracted from each of the fitted values, and Eq. (6) is applied to each corrected phase-shift measurement to produce the plot of gas-fill pressure versus elapsed time depicted in Fig. 52.18(b).

Exponential time constants for the permeation of argon, neon, and deuterium through Al-coated polymer shells were measured using this technique. Figure 52.19 shows results from interferometric measurements taken with a polymer

Fig. 52.17

Typical phase-shift measurements acquired using scanning Fabry-Perot interferometry. (a) The fractional phase shift imposed on light passing through an argon-filled inertial-fusion target as a function of the elapsed time since its removal from the permeation vessel. This polymer shell had a 305- $\mu\text{m}$  outer diameter and consisted of a 3- $\mu\text{m}$ -thick polystyrene shell overcoated with a 3- $\mu\text{m}$ -thick parylene layer. The external argon pressure applied during pressurization was 21.3 atm. (b) The absolute phase shift as a function of elapsed time. Successive integers were added to adjacent groups of fractional phase shift in Fig. 52.17(a) to produce a continuous curve.

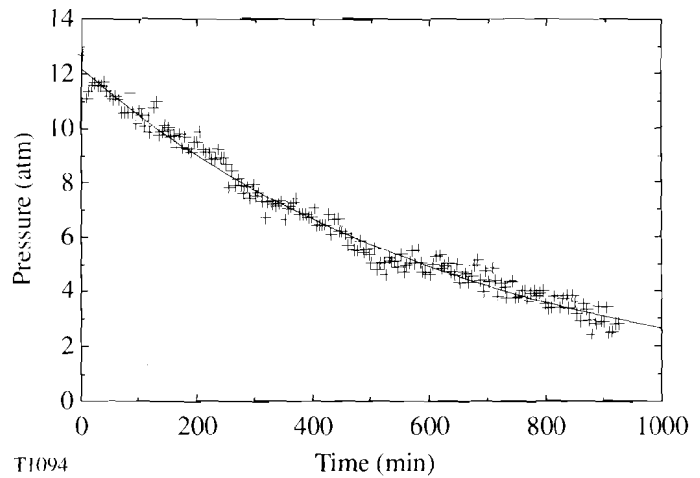




T1032

Fig. 52.18

(a) The least-squares curve fit to the absolute-phase-shift-versus-elapsd-time data given in Fig. 52.17(b). (b) The corresponding least-squares curve fit of its internal pressure versus elapsed time, which was derived from the data given in Fig. 52.17(b). The curve fit yields an initial, internal argon pressure of 19.2 atm and a 30.6-min, exponential-decay time constant.



T1094

Fig. 52.19

The internal pressure of a D<sub>2</sub> shell as a function of time measured with Mach-Zehnder interferometry. This shell was overcoated with a 90-Å-thick Al layer, which produced a time constant of about 11 h.

shell having a 261- $\mu\text{m}$  outer diameter and composed of a 3- $\mu\text{m}$ -thick polystyrene shell overcoated with a 3- $\mu\text{m}$ -thick parylene layer and a 90-Å-thick sputtered Al layer. It was filled by applying an external D<sub>2</sub> pressure of 15.0 atm at room temperature and then allowing it to soak at that pressure for 72 h. The results of the least-squares curve fit for this inertial-fusion target are an initial pressure of 12.2 atm [using  $(n_{\text{gas}} - 1)_{1 \text{ atm}} = (1.29 \pm 0.01) \times 10^{-4} @ \lambda_0 = 488.0 \text{ nm and } 25^\circ\text{C}$  for D<sub>2</sub>],<sup>14</sup> an exponential-decay time constant of 10.9 h, and a residual fractional phase shift of 0.19. The root-mean-squared (rms) deviation of an experimentally

determined phase-shift value from the fitted curve is 0.02, which corresponds to a standard deviation of  $\lambda/50$ . Without aluminum coatings, shells of these dimensions generally have a time constant of only several minutes for  $D_2$ .

Permeation time constants for Al-coated shells of similar dimensions and various Al coating thicknesses are given in Fig. 52.20; included are values for Ar, Ne, and  $D_2$  for the same shells. For the thinner aluminum layers, the time constant varies only slightly between shells from the same batch that were coated simultaneously. However, as the thickness of the Al layer increases, a large shell-to-shell variation in time constant develops. This is assumed to be caused by the formation of aluminum islands on the surface of the shell during the early part of a coating run that coalesce into a continuous film as more material is deposited. The time constant of shells onto which a small amount of aluminum has been deposited is determined by the amount of uncoated surface area that remains between the islands following coating, whereas the time constant of shells that have received thicker, continuous films is defect limited: permeation takes place through regions in the film where its integrity is poor because of surface debris, oily films, stresses in the shell during permeation, etc. Since the amount and severity of defect sites on each shell from a given batch ranges widely, the measured time constants for these shells when simultaneously coated with a thicker layer of Al correspondingly varies, often by as much as  $\pm 30\%$  from their average value.

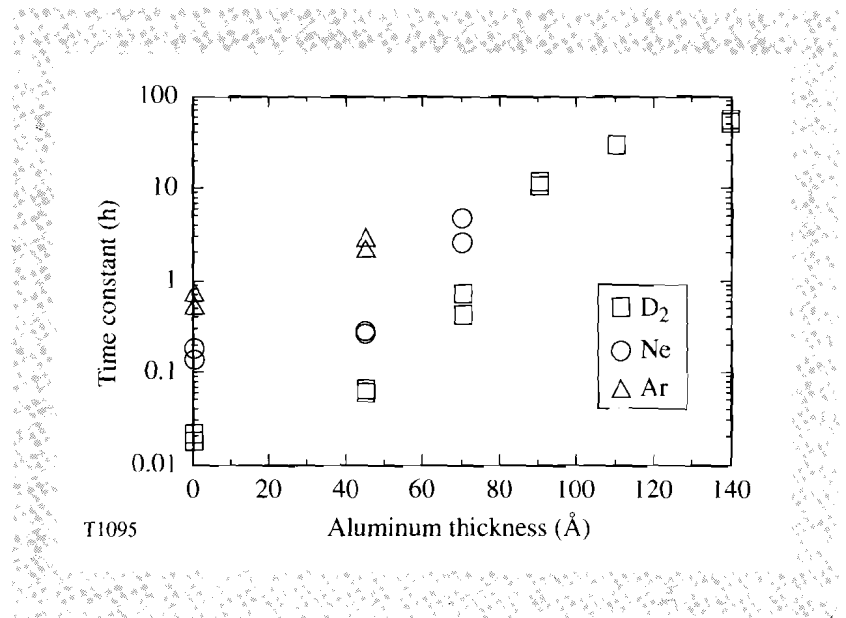


Fig. 52.20 Time constant recorded for gases permeated through shells coated with various thicknesses of Al. All targets were  $250 \pm 10 \mu\text{m}$  in diameter and had  $6\text{-}\mu\text{m}$ -thick polymer walls. For the 45-Å- and 70-Å-thick Al layers, the same shells were permeated and measured using  $D_2$ , Ne, and Ar.

Unlike glass shells, the initial  $D_2$  pressure measured within polymer shells (assuming  $\alpha = 0$ ) is consistently 10% to 20% lower than the pressure at which they were filled, whereas repeated measurements taken with the same shell are reproducible within less than one standard atmosphere. This is a real phenomenon and is not because of inadequacies of the experimental technique used to measure the fill pressure inside a microballoon. For example, in considering the possibility that air permeates back into the shells it is noted that  $n_{\text{gas}} - 1$  for air is about twice

the value for hydrogen at standard conditions. At most, a 2-atm discrepancy between the actual and measured initial fill pressures would occur if air did permeate into the shell during the leakage-rate measurements. Hence, considering the relatively short exponential-decay time constant measured for the hydrogen-containing shell and the comparatively large disagreement between the external pressure applied and that measured, the permeation of air into the polymer shell does not explain the initial pressure discrepancy. The most plausible explanation for this effect is stretching of the shell wall.

When the shell wall stretches because of internal gas pressure, the thinning of the wall produces a change in the original optical phase shift caused by the empty shell that is significant compared to the phase shift caused by the gas. Assuming the stretching of the shell wall is elastic, it shows up as a change in the phase shift through the center of the shell that is proportional to the internal pressure. To predict the magnitude of shell-wall thinning, consider two hemispheres being pushed apart by internal pressure. Assume that the wall thickness  $w$  is much less than the radius  $r$ , so that strain can be treated as uniform throughout the wall. In addition, treat the shell radius as identical to the gas radius. The force trying to separate the two hemispheres  $\pi r^2 P$ , where  $P$  is the internal pressure, acts on an annulus of area  $2\pi r w$ , so that the stress is  $Pr/2w$ . This results in a strain  $\Delta r/r$  given by the ratio of stress to Young's modulus  $Y$

$$\frac{\Delta r}{r} = \frac{Pr}{2Yw} . \quad (7)$$

The change in  $\phi_s$  [Eq. (4)] caused by shell expansion  $\Delta\phi_s$  is independent of the compressibility of the shell. This may be seen by noticing that  $w$  is proportional to  $(\rho r^2)^{-1}$ , where  $\rho$  is the density of the shell material. Since  $n_s - 1$  is, to a good approximation, proportional to  $\rho$ , then  $\phi_s$  is independent of  $\rho$  and is proportional to  $r^{-2}$ . Using this fact, we observe  $\Delta\phi_s = -2\phi_s \Delta r/r$ . Combining this with Eqs. (4) and (7),

$$\Delta\phi_s = \frac{-2mPr(n_s - 1)}{\lambda Y} . \quad (8)$$

The ratio of  $\Delta\phi_s$  to  $\phi_g$  is independent of shell dimensions and pressure and depends only on the refractive indices and Young's modulus. Note that this defines the quantity  $\alpha$  introduced in Eq. (5):

$$\frac{\Delta\phi_s}{\phi_g} = -\frac{P_r}{Y} \frac{(n_s - 1)}{(n_g - 1)} = -\alpha . \quad (9)$$

Using typical values for polystyrene,  $Y = 3200$  MPa,  $n_s = 1.59$ , we find for the gases  $D_2$ , He, Ne, and Ar, values of  $\alpha$  are 0.15, 0.58, 0.30, and 0.07, respectively, at  $\lambda = 546$  nm and a temperature of 25°C. These values can be used to correct the interferometric measurement of phase as a function of time as the gas permeates out of the shell. Precise agreement with these numbers is not expected because the parylene layer has different values of  $Y$  and  $n_s$ .

Inertial-fusion targets containing several gases, each with significantly different permeation time constants, have been made using aluminum gas-barrier layers. For example, various mixtures of  $D_2$  and Ar were permeated into Al-coated polymer shells using the following procedure. The shells are first evacuated by placing them in vacuum overnight, either in the sputter coater's vacuum chamber or a separate, evacuated cell. (The time constant for air to permeate from within a shell with dimensions similar to those in Fig. 52.20 is about 1 h.) They are then coated with 45 Å of aluminum, which yields a time constant of about 2 h for Ar in a shell with a 250- $\mu\text{m}$  outside diameter. The shells are then permeated to the desired partial pressure of Ar. A second Al layer is coated over the first to increase the total time constant to a value acceptable for retaining the  $D_2$ . The thickness of the second Al layer is 80 Å to 90 Å, as determined from data such as that in Fig. 52.20, and this coating is completed within a time interval that is much shorter than the Ar time constant for the first coating, typically in less than 10 min. The shell is then permeated with the appropriate gas mixture. A final 500-Å-thick Al coating that serves as a shinerthrough barrier is applied in a time much less than the time constant for  $D_2$  permeation, and the coated shell is returned to the permeation cell to soak in the gas mixture until it is loaded into the target chamber.

Although the measured time constants for shells from the same batch that were coated simultaneously often vary significantly, especially those with thicker layers of Al, out of the nearly 100 shells tested during the development of this barrier-layer technique, no shells lost gas because of an inexplicable failure of the aluminum layer. Those shells that did fail to hold gas were found to have small cracks in their walls when examined with a high-power optical microscope. We have, therefore, found optically transparent aluminum layers to be an extremely reliable technique for retaining gases within polymer shells for inertial-fusion experiments.

#### ACKNOWLEDGMENT

This work was supported by the U.S. Department of Energy Office of Inertial Confinement Fusion under agreement No. DE-FC03-85DP40200 and by the Laser Fusion Feasibility Project at the Laboratory for Laser Energetics, which is sponsored by the New York State Energy Research and Development Authority and the University of Rochester.

#### REFERENCES

1. J. Nuckolls *et al.*, *Nature* **239**, 139 (1992).
2. U. Kubo, M. Nakatsuka, and M. Tsubakihara, Annual Progress Report, ILE, Osaka University, ILE-APR-79 (1979), p. 177.
3. LLE Review **42**, 70 (1990).
4. A. K. Burnham, J. Z. Grens, and E. M. Lilley, *J. Vac. Sci. Technol. A* **5**, 3417 (1987).
5. R. Q. Gram, C. K. Immesoete, H. Kim, and L. Forsley, *J. Vac. Sci. Technol. A* **6**, 2998 (1988).
6. S. A. Letts, D. W. Myers, and L. A. Witt, *J. Vac. Sci. Technol.* **19**, 739 (1981).